Selective hydrogenation of phenylacetylene on gold nanoparticles

S. A. Nikolaev and V.V. Smirnov

Department of Chemistry, M.V. Lomonosov Moscow State University, 1 Leninskie Gory, 119991, Moscow, Russian Federation. Fax: +7 (495) 932 8846.
E-mail: serge2000@rambler.ru

Abstract

This work investigates 2.5 – 30 nm gold nanoparticles immobilized on Al_2O_3. It shows that they possess high activity and stability in selective hydrogenation of phenylacetylene into styrene from a phenylacetylene-styrene mixture at 423 K. Strong dependences of the activity and selectivity of Au/Al_2O_3 on the gold size were revealed: as the size of supported gold nanoparticles was decreased from 30 to 2.5 nm, the TOF of phenylacetylene hydrogenation increased from 0.028 to 0.142 s^{-1} and the selectivity of styrene formation increased by an order of magnitude. The nature of the identified dependences is discussed in terms of "Geometric" and "Electronic" size-effect points.

Introduction

The industrial interest in the catalytic hydrogenation of phenylacetylene has its origin in styrene polymerization, where pure styrene feedstock is needed to preserve the polymerization catalyst (1, 2). A small amount of phenylacetylene in the feed stream can deactivate it; hence, its selective reduction to less than 10 ppm content is necessary. For this purpose, highly selective Pd-Ag catalysts are commonly used (1). However, their activity and stability are not adequate; hence, searching for more effective catalysts is still a topical task.

It is known that gold nanoclusters exhibit high catalytic activity, stability and selectivity in various chemical reactions (3-5). Moreover, there are numerous papers demonstrating that gold-containing nanocomposites are perfect catalysts for hydrogenation of unsaturated compounds such as 1,3-butadiene, acetylene, pent-1-ene, cyclohexane, α,β-unsaturated aldehydes and prop-1-yne (6-11), but selective hydrogenation of phenylacetylene on supported gold nanoparticles has received little attention (6). Thus, the catalytic hydrogenation of phenylacetylene from phenylacetylene-styrene mixture is still of interest from both scientific and industrial standpoints.

Experimental

Starting materials

Phenylacetylene (Aldrich No. 2086451, 98%) and styrene (Aldrich No. 2028515, 99.5%) were distilled from P_2O_5 in an argon atmosphere. Microspherical γ-Al_2O_3 (IKT-02-6M from OAS "Katalizator", Novosibirsk, S = 138 m^2/g) and α-Al_2O_3 (KN-08 from OAS "Katalizator", Novosibirsk, S = 0,6 m^2/g) were used as a support for nanoparticles. The support was activated by calcination at 350°C for 3 h before use. To prepare catalysts, $HAuCl_4 \cdot H_2O$ ("Aurate," TU 6-09-05-1075-89) with a gold content of 49.04 wt. %, distilled water, and 0.1M aqueous NaOH were used.

Preparation and characterization of gold catalysts

Gold nanoparticles were deposited on Al_2O_3 using a deposition-precipitation technique as described in (12). Briefly, pH of an aqueous solution of $HAuCl_4$ was adjusted to 7.0 by adding aqueous NaOH. Then metal oxide powder was dispersed in the solution with stirring for 1 h to deposit gold hydroxide ($Au(OH)_3$) exclusively on the oxide support surface. The precursor obtained was washed several times to remove sodium and chloride ions, dried for 24 h, and finally calcined in air at 623 K for 3 h. The resulting catalysts were stored in an atmosphere of dry argon.

The gold contents in the resulting samples were determined by atomic absorption spectrometry on a Hitachi 180-80 spectrometer. The metal was preliminarily removed from the support by washing with aqua regia

Table 1

*Results of Catalytic Hydrogenation of Phenylacetylene-Styrene mixtures at 423k**

Run	C(Au) %	d(Au) nm	t h	Molar concentration. % xC_8H_6	xC_8H_8	xC_8H_{10}	(C_8H_6) %	S (C_8H_8)	TOF $*10^{-5}$ s^{-1}
				Au/γ-Al_2O_3					
1	0.02	2.5	0	9.8	90.2	0			
			1	0.01	96.7	3.29	99.9	27.33	-
			2	0.01	96.6	3.39	99.9	26.59	-
			4	0.01	96.7	3.29	99.9	27.33	-
2	0.02	2.5	0	30.2	69.8	0			
			1	16,2	80	3,8	46,36	8.50	14552
			2	16,4	79,6	4	45,36	7.97	14344
			4	16,5	79,2	4.3	45,36	7.35	14241
3	0.37	4.0	0	10.2	89.8	0			
			0.6	0.01	95.1	4.89	99.9	18.31	-
			2	0.01	95.0	4.99	99.9	17.96	-
			4	0.01	92.0	7.99	99.9	11.18	-
4	0.37	4.0	0	29.5	70.5	0			
			4	0.01	88.0	11.99	99.9	5.85	
5	1.8	8.0	0	9.6	90.4	0			
			0.5	0.01	79.4	20.59	99.9	4.31	-
			2	0.01	76.0	23.99	99.9	3.76	-
			4	0.01	70.0	29.99	99.9	3.01	-
6	1.8	8.0	0	32.0	68.0	0	-	-	-
			4	0.01	45.09	54.9	99.9	1.32	-
				Au/γ-Al_2O_3					
7	0.03	4.5	0	10.1	89.9	0			-
			1	0.1	95.11	4.79	99.1	18.51	-
			4	0.05	95.46	4.49	99.5	19.93	-
8	0.03	4.5	0	29	71	0			-
			1	18	76.7	5.3	37.93	5.09	13067
			4	17.6	77.6	4.8	39.31	5.82	13543
9	0.8	21	0	28.1	71.9	0			
			1	13.9	59.3	26.8	50.53	1.35	5535
			4	12.5	60.4	27.1	55.52	1.45	6142
10	2.5	30	0	30.4	69.6	0			
			1	20.8	50.4	28.8	31.58	0.73	2521
			4	20	50	30	34.21	0.77	2868

** Run is the experiment number, C(Au) is the weight percent of gold, d(Au) is the mean particle diameter of gold in the catalyst, τ is the time on stream, $\Delta(C_8H_6)=[\chi_0(C_8H_6)-\chi_i(C_8H_6)]*[\chi_0(C_8H_6)]^{-1}*100\%$ is phenylacetylene conversion, $S(C_8H_8)=[(\chi_0(C_8H_6)-\chi_i(C_8H_6)]*[\chi_0(C_8H_8)]*[\chi_0(C_8H_6)]^{-1}*[\chi_0(C_8H_{10})]^{-1}$ is styrene selectivity, TOF is the turnover frequency calculated as the total amount of phenylacetylene converted per weight of surface gold atoms per second*

(HCl : HNO_3=4 : 1). The relative error of gold content determination was less than 1%.

The TEM observation was performed with a LEO912 AB OMEGA electron microscope with 0.1 nm resolution. For each Au/Al_2O_3 catalyst, 300 particles of supported gold were processed to determine the particle size distribution and mean particle diameters.

Hydrogenation of phenylacetylene-styrene mixture

Catalytic experiments were carried out using a fixed-bed flow reactor. A catalyst or support (1g) was placed in a quartz tube, heated to reaction temperature (318-423 K) for 15 min in a stream of hydrogen at a flow rate of 1.25-1.29 cm^3/min. The reactant gas mixture containing phenylacetylene (10-30 molar percent) and styrene (70-90 molar percent) was passed through the catalyst bed at a flow rate of 200-230 h^{-1}. The reactor effluents were analyzed with a Kristall-Lux-4000 gas chromatograph equipped with a flame ionization detector and a 50-m Thermon capillary column.

Calculations of the catalytic activity and selectivity

Phenylacetylene conversion (C_8H_6) was calculated as $(C_8H_6)=[\chi_0(C_8H_6)-\chi_i(C_8H_6)]*[\chi_0(C_8H_6)]^{-1}*100\%$, where $\chi_0(C_8H_6)$ is the molar concentration of phenylacetylene in the initial

Figure 1

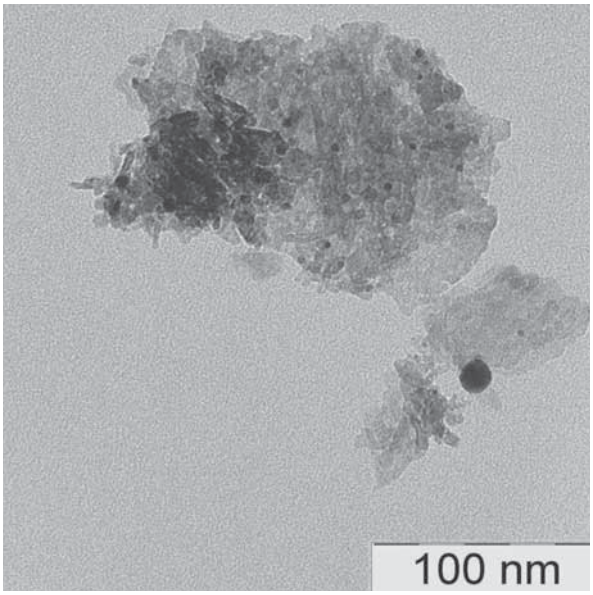

TEM image of the Au/γ-Al_2O_3 (1.8 wt.%) with the maximum of size distribution $d(Au)_{max}$ equal to 8.0±0.1 nm

Figure 2

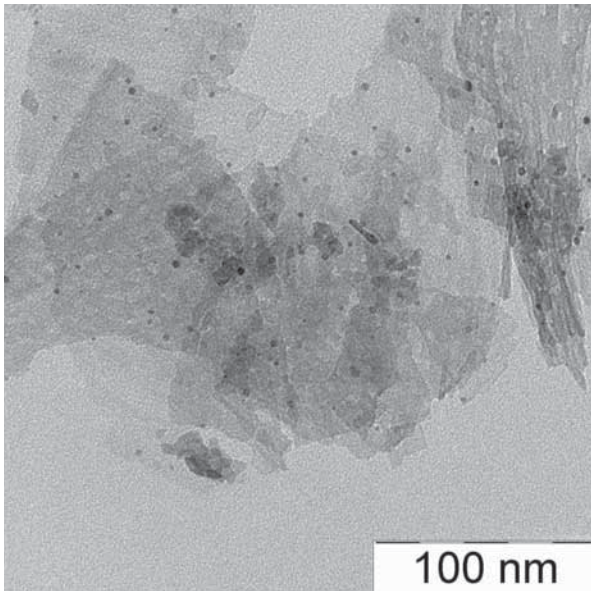

TEM image of the Au/γ-Al_2O_3 (0.37 wt.%) with the maximum of size distribution $d(Au)_{max}$ equal to 4.0±0.1 nm

Figure 3

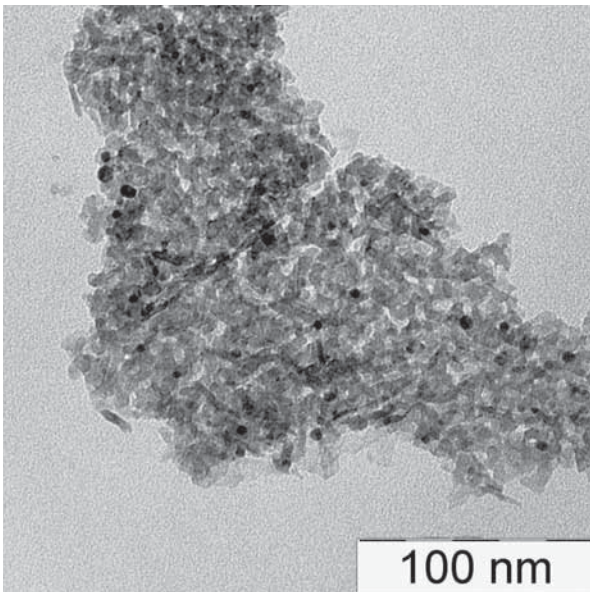

TEM image of the Au/γ-Al_2O_3 (0.02 wt.%) with the maximum of size distribution $d(Au)_{max}$ equal to 2.5±0.1 nm

Figure 4

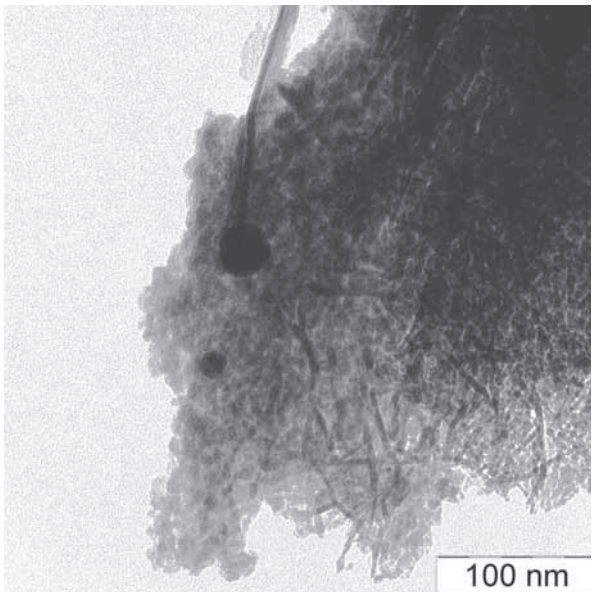

TEM image of the Au/α-Al_2O_3 (2.5 wt.%) with the maximum of size distribution $d(Au)_{max}$ equal to 30.0±0.1 nm

gas mixture, $\chi_i(C_8H_6)$ is the molar concentration of phenylacetylene in the products after *i* hours. The selectivity of the styrene formation was determined as $S(C_8H_8)=[(\chi_0(C_8H_6)-\chi_t(C_8H_6)]*[\chi_0(C_8H_8)]*[\chi_0(C_8H_6)]^{-1}*[\chi_i(C_8H_{10})]^{-1}$, where $\chi_0(C_8H_6)$ and $\chi_0(C_8H_8)$ are the molar concentrations of phenylacetylene and styrene in initial gas mixture, respectively; $\chi_i(C_8H_6)$ and $\chi_i(C_8H_{10})$ are the molar concentrations of phenylacetylene and ethylbenzene in the products after *i* hours, respectively.

The turn-over frequency (TOF) was calculated as $TOF = A*B^{-1}*t^{-1}$ as described previously (7,13,14). Here (A) is the total moles of phenylacetylene converted per total gold surface area (B) per reaction time (t). (B) was calculated as $B = B_{total}\ D$, where (B_{total}) is the total amount of gold in the catalyst sample and (D) is the degree of dispersion for (i.e., the surface-to-volume ratio) gold nanoparticles with different mean diameters d(Au) calculated in (13,14).

Figure 5

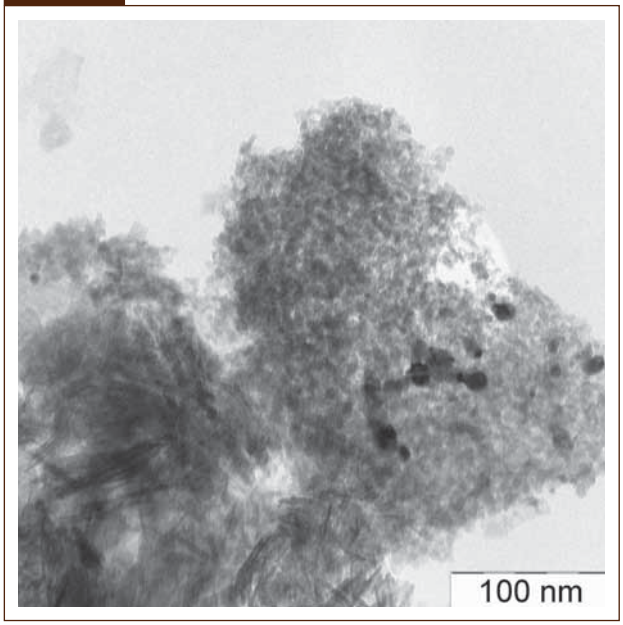

TEM image of the Au/α-Al_2O_3 (0.8 wt.%) with the maximum of size distribution $d(Au)_{max}$ equal to 21.0±0.1 nm

Figure 6

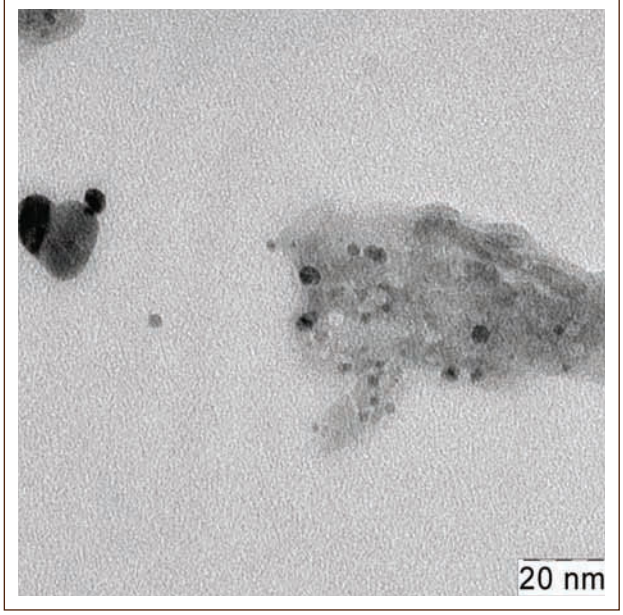

TEM image of the Au/α-Al_2O_3 (0.03 wt.%) with the maximum of size distribution $d(Au)_{max}$ equal to 4.5±0.1 nm

Results and discussion

The color and size of supported on γ-Al_2O_3 gold particles

Three Au/γ-Al_2O_3 catalysts with gold concentrations of 1.8, 0.37 and 0.02 wt. % and three Au/α-Al_2O_3 catalysts with gold concentrations of 2.5, 0.8 and 0.03 wt. % were obtained via deposition-precipitation technique (Table 1). All samples were lilac-colored highly dispersed dry powders. As the metal content in catalysts increased from 0.02 to 2.5 %, the color intensity increased too. The observed color and its variation with gold concentration were in good agreement with data published earlier by Bond (5).

Typical TEM images of the synthesized catalysts are presented in Figs. 1-6. The diameters of detectable gold particles in Au/γ-Al_2O_3 catalysts with 1.8, 0.368 and 0.018 wt.% gold contents were (5-10)±0.1, (3-5)±0.1 and (2-3)±0.1 nm, respectively. The particle diameters in Au/α-Al_2O_3 with 2.5, 0.8 and 0.03 wt.% gold contents were (24-46)±0.1, (16-25)±0.1 and (4-7)±0.1 nm, respectively. The gold size distribution in each sample was sharp and monomodal. At approximately the same gold content, the nanoparticles in Au/α-Al_2O_3 were larger than those in Au/γ-Al_2O_3. This can be attributed to the much smaller surface area of α-Al_2O_3 in contrast with γ-Al_2O_3, which led to more effective aggregation of gold in the calcination stage.

Since the catalytic properties are associated with the surface of supported nanoparticles, the mean particle diameters d(Au) were calculated from the maximum of gold size distributions. The results are summarized in Table 1. From the d(Au) values, the degree of dispersion D (i.e., the surface-to-volume ratio) was estimated, thus enabling the calculation of the TOF.

Catalytic properties of clean γ-Al_2O_3 support in hydrogenation at 423K

Before discussing the results of hydrogenation of phenylacetylene-styrene mixture on immobilized gold nanoparticles, let us briefly review the catalytic behavior of a "clean" support. Control experiments showed that the reactant mixture passed through α- or γ-Al_2O_3 heated to 423K contains ethylbenzene (≤2%); thus, these supports possess a slight hydrogenation activity.

A slight catalytic activity of the support in total hydrogenation of unsaturated compounds is not unusual. For example, Lopez-Sanchez and Mohr mentioned that Fe_2O_3 support is active in hydrogenation of prop-1-yne at 523K (8) and ZrO_2 support catalyzes the hydrogenation of acrolein at 593K (13). Thus, the weak activity of our γ-Al_2O_3 or α-Al_2O_3 support could be explained by trace amount of Fe^{+3} (according to IKT-02-6M certificate, the concentration of Fe may reach 10^{-4} wt. %) or other metals. Unfortunately, we could not reduce the support activity by decreasing the reaction temperature below 423K since this resulted in intensive condensation of phenylacetylene (b.p. = 417K) and styrene (b.p. = 419 K) on the support. In the subsequent processing of experimental data, the support catalytic activity was taken into account.

Hydrogenation of phenylacetylene-styrene mixture on Au/γ-Al_2O_3 at 423K

The results of hydrogenation of the phenylacetylene-styrene mixture on Au/γ-Al_2O_3 and Au/α-Al_2O_3 at 423K are summarized in Table 1: runs 1-6 and 7-10, respectively. No significant

Figure 7

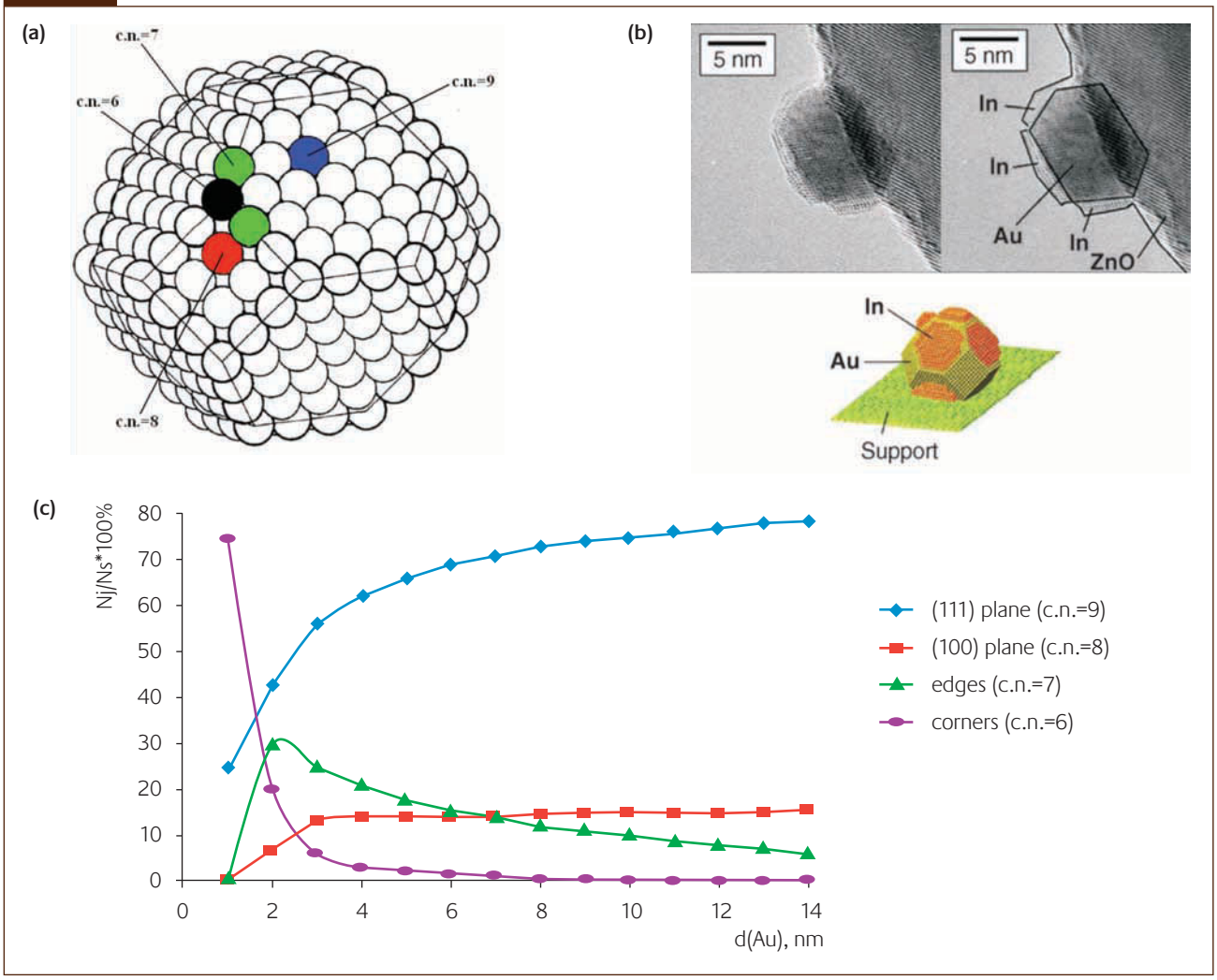

Cuboctahedron model of gold nanoparticle (a) and the dependence of relative numbers of surface sites Nj/Ns on the diameters of cuboctahedron gold particles (b), where Nj is the number of surface atoms with coordination number j, Ns is the total number of surface atoms (as given in (18)). HRTEM image of real Au-In/ZnO catalyst (c). Indium preferentially decorates the outer faces of the gold particles while the edges remain uncovered (as given in 14)

difference was observed between catalytic hydrogenation on the same-size nanoparticles supported on γ-Al_2O_3 or α-Al_2O_3: the conversion, selectivity and stability of these catalysts were approximately equal (Table1, compare run 3 and run 7). Thus, the type of alumina does not influence significantly the catalytic properties of supported gold in this reaction.

Depending on the concentration of phenylacetylene in the initial mixture, its conversion on supported gold nanoparticles at 423 K varied from 30 to 99.99%. During each run, the conversion was constant for at least 4 hours. The observed conversion values are in agreement with the earlier found conversions of other acetylene derivatives on Au/Al_2O_3 prepared via deposition-precipitation (for example, conversion of prop-1-yne at 423K was 50% (8), conversion of acetylene at 453-473K was 40-85% (9,10)). The good working stability found for our catalysts is also in good agreement with published data (9) and can be attributed to the absence of oligomers in the product mixture.

The TOF calculated at approximately equal (30-50%) conversions on 2.5, 4.5, 20 and 30 nm gold nanoparticles in phenylacetylene hydrogenation at 423K are 0.142, 0.135, 0.061 and 0.028 s^{-1} respectively (Table 1, runs 2, 8-10), which, on the whole, is comparable with the TOF on the same-size gold particles supported on different types of Al_2O_3 in hydrogenation of unsaturated compounds (7,15) and is lower than the hydrogenation activity of Pt/Al_2O_3 or Pd/Al_2O_3 (16).

In contrast with traditional metals for hydrogenation (Pd, Rh, Ru, Ni), supported gold nanoparticles possess a unique feature: the activity and selectivity of gold in hydrogenation of unsaturated compounds are strongly dependent on its size. This phenomenon was mentioned repeatedly for 1,3-butadiene and crotonaldehyde (7), acetylene (9,10), pent-1-ene (5), dodec-1-ene (17), acrolein (4,13,18), and naphthalene (19) and it seems that it does not depend on the nature of the unsaturated substrate, a method of catalysts preparation or process temperature (5,6,18). The results of phenylacetylene hydrogenation on the supported gold

nanoparticles presented in Table 1 show that our process is not an exception to the rule.

The catalytic experiments at 30-55% conversion revealed a great increase in the TOF from 0.028 to 0.142 s^{-1} upon a decrease in the particle size from 30 to 2.5 nm (Table 1, runs 2, 8-10). The strong size dependence of the selectivity was also detected: as the size of gold nanoparticles was decreased from 30 to 2.5 nm, the selectivity to styrene S increased by an order of magnitude (Table 1, runs 2, 8-10). In experiments with 100% conversion of phenylacetylene (Table 1, runs 1, 3-6), the TOF values cannot be estimated precisely, but as for S, one can see again that as the size of gold nanoparticles decreased, the selectivity to styrene increased.

The influence of the particle size of the metal on both the TOF and the selectivity are believed to be brought about by "geometric" and/or "electronic" size effects (3-6,18-22). Now we discuss how these effects could be manifested and how we can explain the observed changes in the activity and selectivity

The contribution of "geometric" and "electronic" effects into hydrogenation properties of gold nanoparticles

It is well known that the activity of individual atom on the catalyst surface strongly depends on its environment. The ratio of different types of surface atoms changes substantially with varying the particle size (18,23). Large particles possess mainly large crystal planes with atoms of high coordination number (terrace atoms), whereas metal atoms with low coordination numbers (edge and corner atoms) are characteristic of small particles. Such changes may manifest themselves as "geometric" or "ensemble effect". Of course, this should affect adsorption and reactivity of unsaturated substrates on the surface of the supported nanoparticles.

In equilibrium state, the shape of nano-sized gold should be a cuboctahedron (24). Therefore, we use a cuboctahedron geometrical model of the particle (Fig.7, a) suggested by van Hardefeld and Hartog (23). The dependence of the proportions of various surface atoms on the particle diameter for cuboctahedron model (Fig. 7, b) was calculated by Mohr (18). Of course, this model is approximate; the error in the estimation of the numbers of various surface atoms can be as high as tens of percent. However, since the size effects observed in the present paper are very high, the qualitative conclusions presented below can be considered reliable.

First of all, let us correlate the changes of TOF with the ratio of various types of surface atoms (see Fig.7, b). One can see that as d(Au) decreases, the overall fraction of gold atoms with low coordination number (6 and 7, corner and edge atoms) increases, whereas the fraction of plane atoms with high coordination number (8 and 9) decreases (Fig.7, b). Thus now we can link the increase in the concentration of low-coordinated atoms (Fig.7, b) to the observed increase in TOF in phenylacetylene hydrogenation (Table 1, runs 2, 8-10). As a result, we can propose that corner and edge atoms make the major contribution to the hydrogenation process, i.e., they are the most active part of the gold nanoparticle surface.

An interesting study that fully supports the above thesis was carried out by Mohr and Claus (14). They measured the activity and selectivity of gold nanoparticles, both neat and with indium-decorated faces, in the hydrogenation of acrolein. The TOF of 9.0-nm neat gold nanoparticles and 10-nm gold nanoparticles with indium-decorated gold faces were 0.1 and 0.05 s^{-1} respectively as reported in (14). If we take into account that indium does not possess hydrogenation activity and that after decoration 100% of the surface gold nanoparticle planes and approximately 40-50% of gold nanoparticle edges and corners* were isolated from the reaction, the reported results clearly demonstrate that the most active sites for hydrogenation should be exactly the edge and/or corner gold atoms.

Another piece of evidence for superior activity of corner and edge atoms in contrast to plane atoms was obtained by Bus and Jia. On the basis of careful analysis of Au/Al_2O_3 by *in-situ* X-ray absorption spectroscopy, chemisorption, and H/D exchange experiments, Bus (25) has revealed that only the gold atoms in the corner and edge positions could induce dissociation of hydrogen. The author also found that the average number of the adsorbed hydrogen atoms per surface gold atom increases with decreasing particle size. In his subsequent study of hydrogenation of cinnamaldehyde, he has found that the TOF increased as the total H/Au ratio increased with a decrease in the gold particle size (15). The elucidated dependences of hydrogen chemisorption and TOF in acetylene hydrogenation on the size of supported gold particles obtained by Jia (9) are similar to the results reported by Bus (15,25).

Summarizing the above results we can explain the influence of the "Geometric" effect on the TOF in hydrogenation of a phenylacetylene-styrene mixture: as the gold nanoparticle size decreases, the concentration of surface sites responsible for hydrogenation (edges and corners) increases, and this is manifested in the increase in the rate of the phenylacetylene hydrogenation.

To discuss the role of "Geometric" effect in the dependence of the selectivity on the particle size (Table 1, runs 2, 8-10), first examine the hydrocarbon adsorption on the corners, edges and planes of gold nanoparticles. Outka and Madix studied the adsorption of ethylene and acetylene on Au(110) crystal plane via TPD (4). For both hydrocarbons, a single broad desorption peak between 125-200 K was observed with no signs of decomposition products. Koel and co-workers (4) studied the adsorption properties of cyclohexane and cyclohex-1-ene on Au(111) crystal plane. These substrates have shown similar adsorption behavior: they undergo reversible adsorption without decomposition. The binding energies of dec-1-ene, n-decane, hex-1-ene and

** Although the authors did not mentioned that, the decoration of some edges and corners could be easily seen on their Au-In HRTEM images (Fig. 7c)*

n-hexane on Au(111) crystal plane are 81.1, 80.1, 56.6, 56 respectively (26). There is no significant difference between adsorption of acetylenes, alkenes or alkanes on gold planes. Differences in the adsorption behavior arise as gold planes are replaced by a combination of gold planes, corners and edges. Jia (9) has shown that at 273K, the amount of acetylene adsorbed on 3.8-nm gold particles immobilized on Al_2O_3 was 18 times greater than that of ethylene. Moreover, in contrast to ethylene, adsorption of acetylene was irreversible. Segura (11) demonstrated that 4-nm gold nanoparticles supported on CeO_2 are extremely selective in the hydrogenation of triple bonds in propyne-propene mixtures. The authors DFT simulations proved that the observed selectivity is related to the stronger adsorption of prop-1-yne in contrast with propene on edges of supported gold nanoparticles.

The results described clarify the role of the "Geometric" effect in the dependence of styrene selectivity on particle size observed by our group (Table 1, runs 2, 8-10). As the size of gold particles decreases, the ratio of (corners+edges) to (planes) increases. This leads to essential increase in adsorption of phenylacetylene relative to styrene, which results in an increase in selective hydrogenation of phenylacetylene from alkyne-alkene mixtures. Moreover, according to the classical mechanism of acetylene hydrogenation on palladium (20), diatomic Pd ensembles are required to produce ethylene from acetylene, while tri- and preferably tetraatomic ensembles are necessary for total hydrogenation of acetylene into ethane and for oligomerization. Since tri- and tetraatomic ensembles are characteristic of planes, it can also be said that as the size of nanoparticles decreases, the surface concentration of plane atoms in nanoparticle decreases (Fig.7 a); this reduces the number of tetraatomic ensembles. As a result, side reactions such as complete hydrogenation and oligomerization are suppressed and the selectivity increases.

It is known that electronic properties of metal particles can change appreciably when the number of atoms in an isolated metal particle is reduced. This is so called "electronic" or "ligand effect". There is much evidence to indicate that very small metal particles do not have the band structure characteristic of bulk metals and they appear to be electron deficient (20,21). In other words, as the particle size decreases, the electron deficiency increases. This can have a strong influence on the adsorption behavior by changing (usually increasing) the adsorption energy of unsaturated compounds and increasing the rate of hydrogenation (18). In the supported gold, some supports can behave as electron acceptors or donors and thus affect the adsorption and hydrogenation rate of unsaturated compounds. Electron transfer from the support to gold was found in Au/TiO_2 systems, resulting in a decrease in the C=C bond hydrogenation rate (4-6). In the case of Au/Al_2O_3 catalysts, the situation is opposite: gold nanoparticles supported on alumina are positively charged (4,27,28) and this charge slightly increases as the size of nanoparticles decreases (4). Of course, the chemisorption of electron-rich substrates such as alkynes on gold particles with higher positive charge should be more preferable. The latter should lead to increasing of TOF and S. Alkynes are stronger Lewis bases than alkenes, so their adsorption from alkyne-alkene stream should be more selective. Thus, the "Electronic" size effect can explain the increase in the TOF and selectivity of phenylacetylene hydrogenation from phenylacetylene-styrene mixture observed in this work.

Conclusions

2.5 – 30 nm gold nanoparticles immobilized on alumina possess high activity, selectivity and stability in the hydrogenation of phenylacetylene into styrene from phenylacetylene-styrene mixture. An increase of TOF and selectivity for smaller gold particles was found. This trend can be attributed to the increased surface concentration of corner and edge gold atoms in small particles and/or to increased electron deficiency and positive surface charge of small particles supported on Al_2O_3.

Acknowledgements

This work was supported by the RFBR (grant no. 08-03-00389). S.A. Nikolaev was also supported by the Council of President grants for the young scientists (grant MK-5703.2008.3).

About the authors

Professor Smirnov Vladimir Valentinovich is the Head of Laboratory of Kinetics of Homogeneous Catalytic Reactions at the M.V. Lomonosov Moscow State University (Moscow). His research interest involves homogeneous and heterogeneous catalysis, chemical reaction engineering and new experimental methods to discover catalysts and materials. During his scientific practice he trained 16 PhDs and published about 280 scientific articles.

PhD Nikolaev Sergey Alexandrovich is a young scientist of the M.V. Lomonosov Moscow State University (Moscow) where he specializes in heterogeneous catalysis by metal nanoparticles, mainly in catalysis by gold, palladium and nickel.

References

1 A. Borodziński; G.C. Bond, *Catal. Rev.–Sci. Eng*., 2006, **48**, P.91
2 James T. Merrill, Pat. US 7105711 B2, Fina Technology Ink, 2006
3 M. Haruta, *Gold Bull*., 2004, **37**, P.27
4 R. Meyer, C. Lemire, Sh.K. Shaikhutdinov, H.-J. Freund, *Gold Bull*., 2004, **37**, P.72
5 G.C. Bond and D.T. Thompson, *Catal. Rev.–Sci. Eng*., 1999, **41**, P.319
6 A. Hashmi, K. Stephen, G.J. Hutchings, *Angew. Chem. Int. Ed*., 2006, **45**, P.7896
7 *M. Okumura, T. Akita, M. Haruta, Catal. Today, 2002, **74**, P.265*
8 *J.A. Lopez-Sanchez, D. Lennon, Appl. Catal. A: General, 2005, **291**, P.230*
9 J. Jia, K. Haraki, J.N. Kondo, K. Domen, K. Tamaru, *J. Phys. Chem. B*., 2000, **104**, P.11153
10 T.V. Choudhary, C. Sivadinarayana, A.K. Datye, D. Kumar, D.W. Goodman, *Catal. Lett*., 2003, **86**, P.1
11 Y. Segura, N. López, J. Pérez-Ramírez, *J. Catal*., 2007, **247**, P.383
12 V.V. Smirnov, S.A. Nikolaev, G.P. Murav'eva, L.A. Tyurina, A.Yu. Vasil'kov, *Kinetics and Catalysis*, 2007, **48**, P. 265 [Engl. Transl.]
13 C. Mohr, H. Hofmeister, P. Claus, *J. Catal*. 2003, **213**, P.86
14 C. Mohr, H. Hofmeister, J. Radnik, P. Claus, *J. Am. Chem. Soc*., 2003, **125**, P.1905
15 E. Bus, R. Prins, J.A. van Bokhoven, *Catal. Commun*., 2007, **8** , P.1397
16 G. Del Angel, J.L. Benitez, *React. Kinet. Catal. Lett*., 1993, **51**, No. 2, P. 547
17 V.V. Smirnov, S.A. Nikolaev, L.A. Tyurina, A.Yu. Vasil'kov, *Petroleum Chemistry*, 2006, **46**, No 4, P.296 [Engl. Transl.]
18 C. Mohr, P. Claus, *Science Progress*, 2001, **84**, No 4, P.311
19 B. Pawelec, A.M. Venezia, V. La Parola, S. Thomas, J.L.G. Fierro, *Appl. Catal. A: General*, 2005, **283**, P.165
20 A. Molnar, A. Sarkany, M. Varga. *J. Mol. Catal. A: Chem*., 2001, **173**, P.185
21 V.I. Bukhtiyarov, *Russ. Chem. Rev*, 2007, **76**, No 6, P. 553 [Engl. Transl.]
22 A. Yu. Stakheev, L.M. Kustov, *Appl. Catal. A: General*, 1999, **188**, P.3
23 R. Van Hardeveld, F. Hartog, *Surf. Sci*., 1969, **15**, P.189
24 C.R. Henry, *Surface Science Reports*, 1998, **31**, P.235
25 E. Bus, J.T. Miller, J.A. van Bokhoven, *J. Phys. Chem. B*, 2005, **109**, No 30, P.14581
26 R.J. Baxter, G. Teobaldi, F. Zerbetto, *Langmuir*, 2003, **19**, P.7335
27 C.K. Costello, J.H. Yang, H.Y. Law, Y. Wang, J.N. Lin, L.D. Marks, M.C. Kung, H.H. Kung, *Appl. Catal. A: General*, 2003, **243**, P.15
28 H.H. Kung, M.C. Kung, C.K. Costello, *J. Catal*., 2003, **216**, P.425